112551

/N-92-CR
092741

CGRO GUEST INVESTIGATOR PROGRAM

PROGRESS REPORT FOR GRANT NAG 5-2420:

"EGRET HIGH ENERGY CAPABILITY" and "MULTIWAVELENGTH FLARE STUDIES"

AND GRANT NAG 5-3518: "SOLAR FLARE PROTON SPECTRA"

Principal Investigator: Dr. Edward L. Chupp

Period Covered by Report: 11/15/96 – 11/15/97

Space Science Center, University of New Hampshire, Durham NH 03824

The study of EGRET/TASC flare data has been funded during phases 3–6 of the CGRO Guest Investigator program. The funding and accomplishments can be summarized as follows:

Phase 3. – Under PI Dr. David L. Bertsch (GSFC) the proposal "Use of EGRET High-Energy Capability to Investigate Energetic Solar Flare Processes" was funded with E. L. Chupp and P. P. Dunphy as Co-Investigators at a level of $15,500 instead of the $22,000 requested (NAG 5-2420).

Under *Phase 3* support the accomplishments were:

UNH was assigned the responsibility to use their accelerator neutron measurements to verify the *TASC* response function and to modify the *TASC* fitting program to include a high energy neutron contribution. Direct accelerator-based measurements by UNH of the energy-dependent efficiencies for detecting neutrons with energies from 36 to 720 MeV in NaI were compared with Monte Carlo TASC calculations. The calculated TASC efficiencies are somewhat lower (by about 20%) than the accelerator results in the energy range 70–300 MeV. The measured energy-loss spectrum for 207 MeV neutron interactions in NaI were compared with the Monte Carlo response for 200 MeV neutrons in the TASC indicating good agreement. Based on this agreement, the simulation was considered to be sufficiently accurate to generate a neutron response library to be used by UNH in modifying the *TASC* fitting program to include a neutron component in the flare spectrun modeling. *TASC* energy-loss data on the 1991 June 11 flare was transferred to UNH.

Phase 4. – Under PI Dr. E. L. Chupp the proposal "Study of High Energy Neutrons and Gamma-Rays Using the *EGRET* /TASC" was funded at a level of $30,000 (Supplement 1) while the level requested for the proposed work was \$49,000. Under PI Dr. David L. Bertsch the proposal "Investigation of Energetic Solar Flare Processes Using the High Energy Capabilities of *EGRET*" provided UNH Co-Investigators Chupp and Dunphy with \$16,796 of additional funding (Supplement 2) to continue the work started under the phase 3 program instead of the requested amount of \$25,000.

Under *Phase 4* the accomplishments were:

The *Phase 3* effort to determine a high energy neutron contribution to the emissions from the 1991 June 11 solar flare was continued. A preliminary upper limit to the neutron fluence (> 50 MeV) from this flare was found by adding a theoretical solar neutron spectrum to the TASC spectral fit program. The result was <27 neutrons cm^{-2} which corresponds to $< 2.2 \times 10^{28}$ neutrons sr^{-1} (> 50 MeV) emitted from the Sun toward the Earth. This is about a factor of 10 less than the neutron emissivity from the 1982 June 3 solar flare. This result was presented by P. P. Dunphy, E. L. Chupp, D. L. Bertsch, E. J. Schneid, and S. Gottesman at the 24th International Cosmic Ray Conference at Rome in September 1995. Subsequently, the *TASC* spectral fitting program has been modified to include components from: γ-ray lines (solar and background), bremsstrahlung, neutral pion decay and high energy neutron interactions.

The next step in the analysis of this event, was doing full fits to the *TASC* energy-loss spectra as a function of time. A significant hardening of the solar proton spectrum over time was found for the flare. The results from the analysis were presented at the 188th meeting of the AAS in Madison, WI by P. P. Dunphy *et al.* in June 1996.

Phase 5. – Under PI Dr. E. L. Chupp the proposal "Multiwavelength Studies of October 91 X-Class Solar Flares Observed by EGRET" was funded at a level of \$15,000 (Supplement 3) instead of the \$52,000 requested.

Under *Phase 5* the accomplishments and ongoing work are:

For the *Phase 5* work, we have gathered a significant amount of correlated data for flares observed by the EGRET/TASC. This includes the TASC spectral data for 5 X–class flares between 1991 October 21 and 1991 November 3, as well as the corresponding response functions which account for the solar angle and the spacecraft mass. Also obtained were: Yohkoh HXT time histories and images for the 1991 October 27 flare, Yohkoh GRS time histories and gamma-ray line spectra for the 1991 October 27 flare, standard GOES x-ray data and NOAA radio reports, Nobeyama radio reports, and Chinese Academy of Sciences Solar-Geophysical Data. Work on this data, with emphasis on the flare of 1991 October 27 is ongoing.

Phase 6. – Under PI Dr. E. L. Chupp the proposal "Characterization of Solar Flare Proton Spectra Using EGRET/TASC Data" was funded at a level of $25,000 (NAG 5-3518).

Under *Phase 6* the accomplishments and ongoing work are:

The goal of the *Phase 6* program is to apply the analysis technique used successfully with the *EGRET / TASC* energy-loss spectra for the 1991 June 11 flare to data on the remaining X-class flares observed in 1991 June as funding permits. The first priority was to use the results from fitting the June 11 flare spectra to constrain the flare proton spectral shape and intensity. Our results to date demonstrate that the TASC spectral analysis contributes crucial information on the particle spectrum interacting at the Sun. A preliminary draft of a paper describing this analysis is attached as an Appendix. We plan to submit the paper to a refereed journal by the end of this year. The next step in the work will be to use a similar analysis on the flare of 1991 June 4.

GAMMA-RAYS AND NEUTRONS AS A PROBE OF FLARE PROTON SPECTRA: THE SOLAR FLARE OF 11 JUNE 1991

Philip P. Dunphy[1], Edward L. Chupp[2], David L. Bertsch[3],

Edward J. Schneid[4], Stephen R. Gottesman[5], and Gottfried Kanbach[6]

[1]*Space Science Center, University of New Hamphire, Durham, NH 03824*

[2]*Physics Department, University of New Hampshire, Durham, NH 03824*

[3]*Laboratory for High Energy Astrophysics, Goddard Space Flight Center, Greenbelt, MD 20771*

[4]*Northrup Grumman, Bethpage, NY 11714*

[5]*Northrup Grumman, Baltimore, MD 21203*

[6]*Max-Planck-Institut für Extraterrestrische Physik, 85740 Garching, Germany*

1 INTRODUCTION

The likelihood of the significant production of measurable fluxes of gamma-rays and neutrons in solar flares was investigated by a number of workers, long before the relevant observations were available (e.g., Fireman 1963; Chupp 1963; Dolan and Fazio 1965). The potential value of gamma-ray and neutron measurements as a probe of energetic ions generated in solar flares was pointed out and expected fluxes were calculated in detail by Ramaty and Lingenfelter (1967) and Lingenfelter (1969). The role of neutrons directly detected at 1 AU and gamma-rays from pion (π) decay were seen to be directly related to very energetic ions, because of the high threshold kinetic energy required for their production ($\sim$ 300 MeV for both π's and neutrons in p–p reactions).

Solar flare neutrons were first detected directly by the SMM spectrometer on 21 June 1980 (Chupp *et al.* 1985). Evidence of pion-decay gamma-rays from the same flare was reported by Forrest *et al.* (1985). Several such satellite-based observations have since been made by SMM (Chupp *et al.* 1987), GAMMA-1 (Akimov 1991, 1994a,b), and Comptel/CGRO (Ryan *et al.* 1994; Rank *et al.* 1994, 1997). The effects of highly energetic neutrons have also been seen by ground-based neutron monitors from a few flares (Debrunner *et al.* 1983; Smart *et al.* 1990; Shea *et al.* 1991; Takahashi *et al.* 1991; Muraki *et al.* 1991; Chiba *et al.* 1992). In the present paper, we report on an analysis of the response of the EGRET Total Absorption Shower Counter (TASC) on the Compton Gamma Ray Observatory to the solar flare of 11 June 1991. We argue that the high-energy emission ($>$ 10 MeV) detected by the TASC in the later stages of the flare is dominated by pion-decay gamma-rays and neutrons. The appearance of this emission marks a significant change in the spectral shape of the protons that interact in the solar atmosphere.

2 DESCRIPTION OF THE EGRET/TASC

The EGRET (Energetic Gamma Ray Experiment Telescope) is a large gamma–ray detector comprising a spark chamber, a NaI(Tl) scintillator/calorimeter, and an anticoincidence plastic scintillator dome. EGRET was designed primarily as a telescope to image 20 MeV to 30 GeV gamma–rays from cosmic sources with high sensitivity. The NaI calorimeter, or TASC, is a large ($76 \times 76 \times 20$ cm^3) spectrometer which measures the total energy of gamma–rays detected by EGRET. The TASC also has a burst/solar flare mode that records spectra in the energy range of 1 to 200 MeV every 32.75 s independent of the spark chamber and the anticoincidence dome. More information about the EGRET detector system can be found in Hughes *et al.* (1988), Kanbach *et al.* (1989), and Thompson *et al.* (1993).

Because of its large volume and mass, the TASC has a high efficiency for detecting solar flare gamma–rays and neutrons > 10 MeV. The EGRET, as well as the other detectors aboard CGRO, are not normally pointed at the Sun, except for times of high solar activity when the Sun is chosen as a target of opportunity. Therefore the response of the TASC to solar gamma–rays and neutrons depends on the orientation of CGRO during a particular flare. This response can be calculated using a "mass model" that accounts for the effects of material throughout the CGRO spacecraft. The response to gamma–rays is calculated using a standard Monte Carlo code for high–energy gamma-rays, EGS4 (Nelson 1985). The response to neutrons is calculated with an analogous code for neutrons, CALOR (Jensen 1990).

Figure 1 shows the calculated energy–loss spectrum in the TASC from 200 MeV neutrons. To check the accuracy of the neutron response code, we have compared this sample calculation with an energy–loss spectrum measured in a large NaI scintillation detector exposed to a tagged neutron beam at 207 MeV (Dunphy *et al.* 1989). The comparison shows good agreement with deviations no more than about 20% from 10 to 200 MeV.

3 DESCRIPTION OF THE OBSERVATIONS AND ANALYSIS

The solar flare of 11 June 1991 was one of a series of flares from active region 6659 that took place during June 1991. Following the occurrence of two GOES X-class flares on 4 June and 6 June, the CGRO instruments were pointed at the Sun. As a result, the active region was close to the EGRET pointing axis (zenith angle = 14°) during the 11 June flare. This flare, which was categorized as GOES class X12, was located at 31°N and 17°W in heliocentric coordinates (Solar Geophysical Data).

Figure 2 shows the response of the EGRET/TASC detector to the flare emission over a range of energy losses from 2 to 200 MeV. The net counting rate due to the flare (32.75 s time bins) has been determined by subtracting background measured approximately 24 hours before and after the flare, when the orbital and geomagnetic conditions were similar. A significant flare contribution was present from about 01:59 UT until 02:39 UT. The counting rate profile shows several distinctive features over this time period: two relatively short bursts from 01:59 - 02:10, an interval of low counting rate from 02:10 - 02:13, and an extended excess after 02:13. For purposes of analysis, we identify the first interval as phase I, the second as the interphase, and the third as phase II. Phases I and II are similar to ones defined by Mandzhavidze *et al.* (1996) for this flare, as we discuss below. Phase I can be subdivided according to the two bursts into time periods of 01:59 - 02:03 (phase I-1) and 02:03 - 02:10 (phase I-2). These time intervals are shown in Figure 2 and listed in Table 1. We note that the sharpness of time structure is limited by the TASC time resolution of 32.75s. The separation of the data into these phases can also be justified directly from a comparison of the "hardness" of the energy–loss spectrum for each phase. To specify the hardness, we compare the TASC counting rate in the energy–loss range 30–200 MeV to the rate in the range 4–8 MeV. These rates and their ratios are shown in Table 1. The ratio R(30-200)/R(4–8) is seen to be more than an order of magnitude greater in phase II compared to the bursts of phase I, implying a significant change in the parent particle spectra.

To specify the details of the spectral changes with time, we fit the energy–loss spectrum for each phase with a multi–component model gamma–ray and neutron spectrum. There are five gamma–ray components: (1) a power law in energy, assumed to be due to electron bremsstrahlung; (2) a line spectrum from nuclear de–excitation; (3) a line at 2.223 MeV from neutron capture by protons; (4) a spectrum (dominated by lines at $\sim$ 7.6 MeV) from activation of Fe nuclear levels by neutrons in the spacecraft; and (5) a broad "line" peaking at 67 MeV from π^0 decay plus a continuum due to bremsstrahlung from electrons and positrons from $\pi^{\pm}$ decay. For the neutron spectrum, two types of spectral shapes are used: (1) a neutron spectrum calculated to be produced by protons with a power law spectrum in energy (Murphy *et al.* 1987) and (2) a neutron spectrum calculated to be produced by protons with a Bessel function spectrum (Murphy *et al.* 1987). These proton (and therefore, neutron) spectral shapes are related to different proton acceleration mechanisms (Murphy *et al.* 1987).

The components of the model are folded through the gamma–ray and neutron response functions described above and fit to the observed energy–loss spectra using a standard Levenberg–Marquardt non–linear multi–parameter iterative fitting routine (Press *et al.* 1989). The results of the fitting procedure are shown in Figure 3. Taking each phase in turn, we point out a number of features. The spectra from the two bursts during phase I are quite similar, with a power–law continuum, a significant contribution from the nuclear line de–excitation component (apparent mainly in the energy range 4–8 MeV), and a strong neutron–capture line at 2.2 MeV. During this phase, there is no significant contribution from pion–decay gamma–rays, solar neutrons, or Fe activation. In fact, these components were omitted from the phase I fits shown in Figure 3. The fit to the interphase has only two significant components: a power–law continuum and the 2.2 MeV neutron–capture line. Again, no pion–decay or neutron component is used in the fit. Finally, the fit to the phase II spectrum indicates a significant pion–decay and/or neutron component but no significant power–law component. Otherwise, this fit requires all of the gamma-ray components listed above. Unfortunately, the response of the EGRET/TASC is very similar for both pion–decay gamma–ray spectra and high–energy neutron spectra. Therefore, we have used combinations of pion–decay and neutron spectra based on theoretical calculations (Murphy and Ramaty 1985). The best–fit parameters and associated uncertainties for each of the phases are listed in Table 2. In the following section, we discuss the implications of the differences between the spectra.

4 RESULTS AND DISCUSSION

One of the most obvious features of the evolution of the high–energy emission from this flare is the clear hardening of the detected spectrum between phases I and II. This can be seen both in the spectral hardness ratios in Table 1 and in the change in spectral shape in Figure 3, where an intensification in the spectrum above 10 MeV occurs during phase II. In our fitting model, this implies a flux of solar neutrons and pion–decay gamma–rays which were not present earlier. Mandzhavidze *et al.* (1996) have already pointed out the change in spectral shape. In fact, the change in shape is more radical than their analysis would imply. Since spectral analysis of the TASC data was beyond the scope of their paper, they had assumed that the emission detected >10 MeV in phase I was due to pion decay. The present spectral analysis indicates that this energy range is actually dominated by electron bremsstrahlung. Thus the change in spectral shape is due to the appearance of a pion–decay component. This, in turn, is due to the hardening of the ion spectrum that produces the nuclear lines and the pion–decay emission.

The virtual disappearance during the interphase of nuclear lines that are a signature of ion interactions imply that the phase I and phase II emissions are, to some extent, independent. This could mean that the ion acceleration mechanisms or the sites of the acceleration are different. The presence of a strong 2.2 MeV neutron–capture line during the interphase is not inconsistent with a decrease in ion interactions, since neutron capture line emission is expected to be delayed with respect to the de–excitation lines (Prince *et al.* 1983; Hua and Lingenfelter 1987).

Using the best–fit neutron and gamma-ray spectral parameters obtained from each phase of the flare, fluences for various components can be calculated, and these are listed in Table 3. These fluences can be applied to appropriate solar gamma–ray and neutron production models (e.g., Murphy and Ramaty 1985; Murphy *et al.* 1987) to constrain the flare proton spectrum. In particular, the relative fluences of the 2.2 MeV line ($F_{2.2}$), the nuclear line emission in the range 4–7 MeV (F_{4-7}), and π^0–decay gamma–rays (F_{π^0}) can be used to constrain the energy spectrum of solar protons that produce these emissions. In Figure 4, we plot the relevant ratios, $F_{2.2}/F_{4-7}$ andF_{π^0}/F_{4-7}, as a function of proton spectral shape, based on calculations by Murphy and Ramaty (1985). From these plots we see that the proton spectral shape is consistent with a Bessel function parameter of 0.019$\pm$0.005 for phase I-1 and 0.028$\pm$0.005 for phase I-2, but inconsistent with a power law. In contrast, the phase II proton spectral shape is consistent with a power–law spectrum with index 2.8$\pm$0.2, but inconsistent with a Bessel function shape. This evolution in ion spectral shape is reminiscent of the flare of 3 June 1982. In that case, Murphy *et al.* (1987) argued that the initial burst of gamma–rays (and neutrons) was due to ion acceleration by a 2nd–order Fermi process, while the time–extended emission was caused by shock acceleration.

We conclude by noting a more general similarity of the high–energy time history of this flare with other large flares. In particular, the presence of an initial impulsive phase (phase I here), followed by a "delayed" or "extended" phase with a harder ion spectrum (phase II here), appear to be the rule rather than the exception for the largest X-class flares detected by SMM, CGRO, and GAMMA-1 (Dunphy and Chupp 1994; Akimov *et al.* 1991, 1994a, 1994b; Ryan *et al.* 1994). It is already known that electrons (> 1 MeV) and ions (> 100 MeV) can be accelerated together over short time scales (~1 s) (Forrest and Chupp 1983; Kane *et al.* 1986). Thus, acceleration models that produce bursts on even shorter time scales than those in phase I have been addressed (references). Models that explain particle acceleration and/or trapping with emphasis on ions which would be appropriate to the phase II emission reported here have also been put forward (Ryan and Lee 1991; Kocharov *et al.* 1993; Guglenko *et al.* 1990; Mandzhavidze *et al.* 1996). Given the commonness of extended phase emission, models which do not depend on unusual or special conditions at the flare site should be favored.

5 ACKNOWLEDGEMENTS

The authors gratefully acknowledge support from NASA through grant NAG 5-2420 (UNH) and contract NAS 5-31210 (Northrup Grumman).

6 REFERENCES

Akimov, V. V. , *et al.* , Proc. 22nd Int. Cosmic Ray Conf. (Dublin) **3**, 73 (1991).

Akimov, V. V., *et al.* , in J. M. Ryan and W. T. Vestrand (eds.), High-Energy Solar Phenomena, AIP, New York, 106 (1994a).

Akimov, V. V., Leikov, N. G., Kurt, V. G., and Chertok, I. M., in J. M. Ryan and W. T. Vestrand (eds.), High-Energy Solar Phenomena, AIP, New York, 130 (1994b).

Chiba, N., *et al.* , Astroparticle Phys. **1** 27 (1992).

Chupp, E. L., in W. N. Hess (ed.), AAS-NASA Symposium on the Physics of Solar Flares, NASA SP-50, 445 (1963).

Chupp, E.L., *et al.* , ApJ (Letters) **273**, L95 (1982).

Chupp, E.L., *et al.* , ApJ **318**, 913 (1987).

Debrunner, H., Flückiger, E., Chupp, E. L., and Forrest, D. J., Proc. 18th Int. Cosmic. Ray Conf. **4**, 75 (1983).

Dolan, J. F. and Fazio, G. G., Rev. of Geophys. **3**, 319 (1965).

Dunphy, P. P., and Chupp, E. L., in J. M. Ryan and W. T. Vestrand (eds.), High-Energy Solar Phenomena, AIP, New York, 112 (1994).

Dunphy, P. P., *et al.* , Experimental Astrophys. **2**, 233 (1989).

Fireman, E. L., in W. N. Hess (ed.), AAS-NASA Symposium on the Physics of Solar Flares, NASA SP-50, 279 (1963).

Forrest, D. J., and Chupp, E. L., Nature **305 (59)**, 291 (1983).

Forrest, D. J. *et al.* , Proc. 19th Int. Cosmic. Ray Conf. **4**, 146 (1985).

Guglenko, V. G., *et al.* , ApJ (Supplement) **73**, 209 (1990).

Hua, X.-M., and Lingenfelter, R.E., ApJ **323**, 779 (1987).

Hughes, E. B. *et al.* , IEEE Trans. Nucl. Sci. **NS-27**, 364 (1988).

Jensen, C. M., CALOR/VAX Users Manual, Applied Science Corporation, Landover, MD (1990).

Kanbach, G. *et al.* , Proc. of the Gamma Ray Observatory Workshop, 2–1 (1989).

Kanbach, G. *et al.* , A & A Suppl. Series **97**, 349 (1993).

Kane, S. R., *et al.* , ApJ (Letters) **300**, L95 (1986).

Kocharov, G. E., *et al.* , Proc. 23rd Int. Cosmic Ray Conf. **3**, 123 (1993).

Lingenfelter, R. E., Sol. Phys. **8**, 341 (1969).

Lingenfelter, R. E. and Ramaty, R., in B. S. P. Shen (ed.), High–Energy Nuclear Reactions in Astrophysics, W. A. Benjamin, Inc., New York, 99 (1967).

Mandzhavidze, N., and Ramaty, R., ApJ **389**, 739 (1992).

Mandzhavidze, N., and Ramaty, R., Nuclear Physics B. Proc. Suppl. **33**, 141 (1993).

Mandzhavidze, N., Ramaty, R., Bertsch, D. L., and Schneid, E. J., *** (1996).

Muraki, Y., *et al.* , ICCR–Report-248-91-17, ICCR, Univ. of Tokyo (1991).

Murphy, R. J. and Ramaty, R., Advances in Space Research **4** #7, 127 (1985).

Murphy, R. J., Dermer, C. D., and Ramaty, R., ApJ Suppl. **63**, 721 (1987).

Nelson, W. R., The EGS4 Code System, SLAC–265, Stanford Linear Accelerator Center, December (1985).

Press, W. H. *et al.* , Numerical Recipes: The Art of Scientific Computing, Cambridge University Press, Cambridge, pp. 523–528 (1989).

Prince, T. A., *et al.* , Proc. 18th Int. Cosmic Ray Conf. **4**, 79 (1983).

Rank, G., *et al.* , in J. M. Ryan and W. T. Vestrand (eds.), High–Energy Solar Phenomena, AIP, New York, 100 (1994).

Rank, G. *et al.* , Proc. 25th Int. Cosmic Ray Conf. **, 5 (1997).

Ryan, J. M., and Lee, M. A., ApJ **368**, 316 (1991).

Ryan, J. M., *et al.* , in J. M. Ryan and W. T. Vestrand (eds.), High–Energy Solar Phenomena, AIP, New York, 89 (1994).

Shea, M. A., Smart, D. F., and Pyle, K. R., Geophys. Res. Letters **18**, 1655 (1991).

Smart, D. F., *et al.* , ApJ (Supplement) **73**, 269 (1990).

Solar Geophysical Data.

Takahashi, K., *et al.* , Proc. 22nd Int. Cosmic Ray Conf. **3**, 37 (1991).

Thompson, D. J., *et al.* , Ap. J. Suppl. Ser. **86**, 629 (1993).

Table 1
Time Intervals and Hardness Ratio for Flare of 1991 June 11

Phase	Start Time	End Time	R(4–8)	R(30–200)	R(30–200)/R(4–8)
I-1	01:59:15	02:03:06	2610±74	1.21±0.84	$4.6(\pm 3.2) \times 10^{-4}$
I-2	02:03:06	02:09:39	3317±52	1.41±0.58	$4.3(\pm 1.8) \times 10^{-4}$
Interphase	02:09:39	02:12:56	269±78	0.61±0.79	-
II	02:12:56	02:40:13	341±12	3.54±0.13	$1.04(\pm 0.05) \times 10^{-2}$

Table 2
Fitting Parameters for Flare of 1991 June 11

Parameter	I–1	I–2	Interphase	II
p.l. index	2.10±.12	2.32±.04	2.20±0.17	—
p.l. coeff.	0.23±.04	0.56±.03	0.16±.04	**0**
nucl. coeff.	1.32±.08	1.61±.06	< 0.097	0.111±.007
2.2 MeV coeff.	0.067±.004	0.157±.003	0.042±.004	0.0186±.0007
Fe line coeff.	$< 1.4 \times 10^{-3}$	$< 9.2 \times 10^{-4}$	$< 1.8 \times 10^{-3}$	$(1.2 \pm .2) \times 10^{-3}$
pion coeff.	$< 2.3 \times 10^{-5}$	$< 9.0 \times 10^{-6}$	**0**	$(5.30 \pm .13) \times 10^{-5}$
neutron coeff.	**0**	**0**	**0**	$\mathbf{5.3 \times 10^{-5}}$

Note: Upper limits are 1σ. Values in bold print were held fixed.

Table 3
Fluences and Proton Spectral Parameters

Phase	F_{4-7}	$F_{2.2}$	F_{π^0}	$F_{2.2}/F_{4-7}$	F_{π^0}/F_{4-7}	αT	s
I-1	21.7±1.8	19.8±1.2	< 0.063	0.91	< 0.029	0.019	—
I-2	43.5±2.3	72.8±1.4	< 0.044	1.67	< 0.010	0.028	—
II	13.1±0.8	30.1±1.1	17.5±0.4	2.30	1.34	—	2.8

Note: Upper limits are 1σ. Fluence units are cm^{-2}.

FIGURE CAPTIONS

Figure 1. Monte Carlo simulation of the response of the EGRET/TASC to 200 MeV neutrons. Responses to both a cylindrical beam of neutrons which extends outside the EGRET envelope (solid line) and a thin pencil beam (dashed line) are shown.

Figure 2. Time history of the response of the TASC during the flare of 11 June 1991 in several energy–loss bands. Background has been subtracted. Demarcations of the phases discussed in the text are shown.

Figure 3. Plots of the energy–loss spectra (background subtracted) observed by the TASC. The spectra were fit with a multi–component model spectrum described in the text.

Figure 4. The fluence ratios $F_{2.2}/F_{4-7}$ and F_{π^0}/F_{4-7} are plotted for two proton spectral shapes: (a) a Bessel function in energy characterized by parameter αT and (b) a power law in energy with index -s. The curves are theoretical values based on calculations by Murphy and Ramaty (1985). The thickened sections correspond to the values observed for 3 time periods (I-1, I-2, and II) during the flare of 11 June 1991.

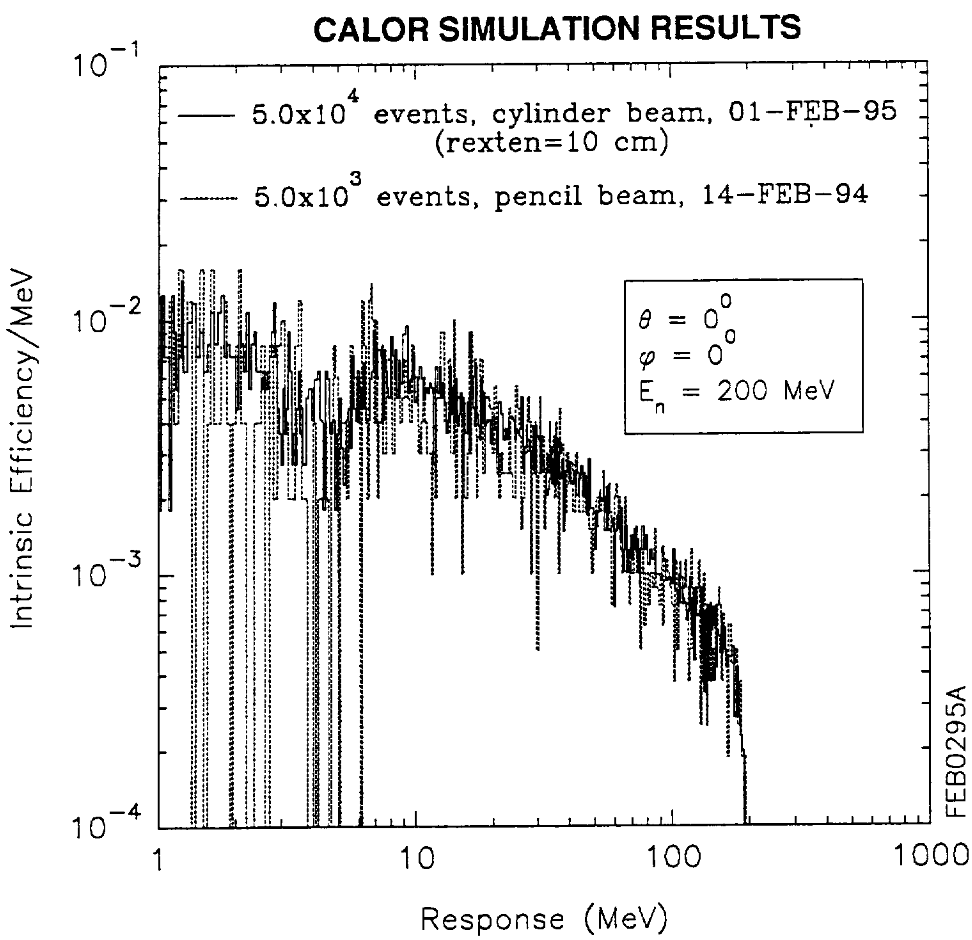

CALOR SIMULATION RESULTS
5.0x10^4 events, cylinder beam, 01-FEB-95
(rexten=10 cm)
5.0x10^3 events, pencil beam, 14-FEB-94
θ = 0^0
φ = 0^0
E_n = 200 MeV
Intrinsic Efficiency/MeV
Response (MeV)
10^-1
10^-2
10^-3
10^-4
1
10
100
1000
FEB0295A

Figure 1.

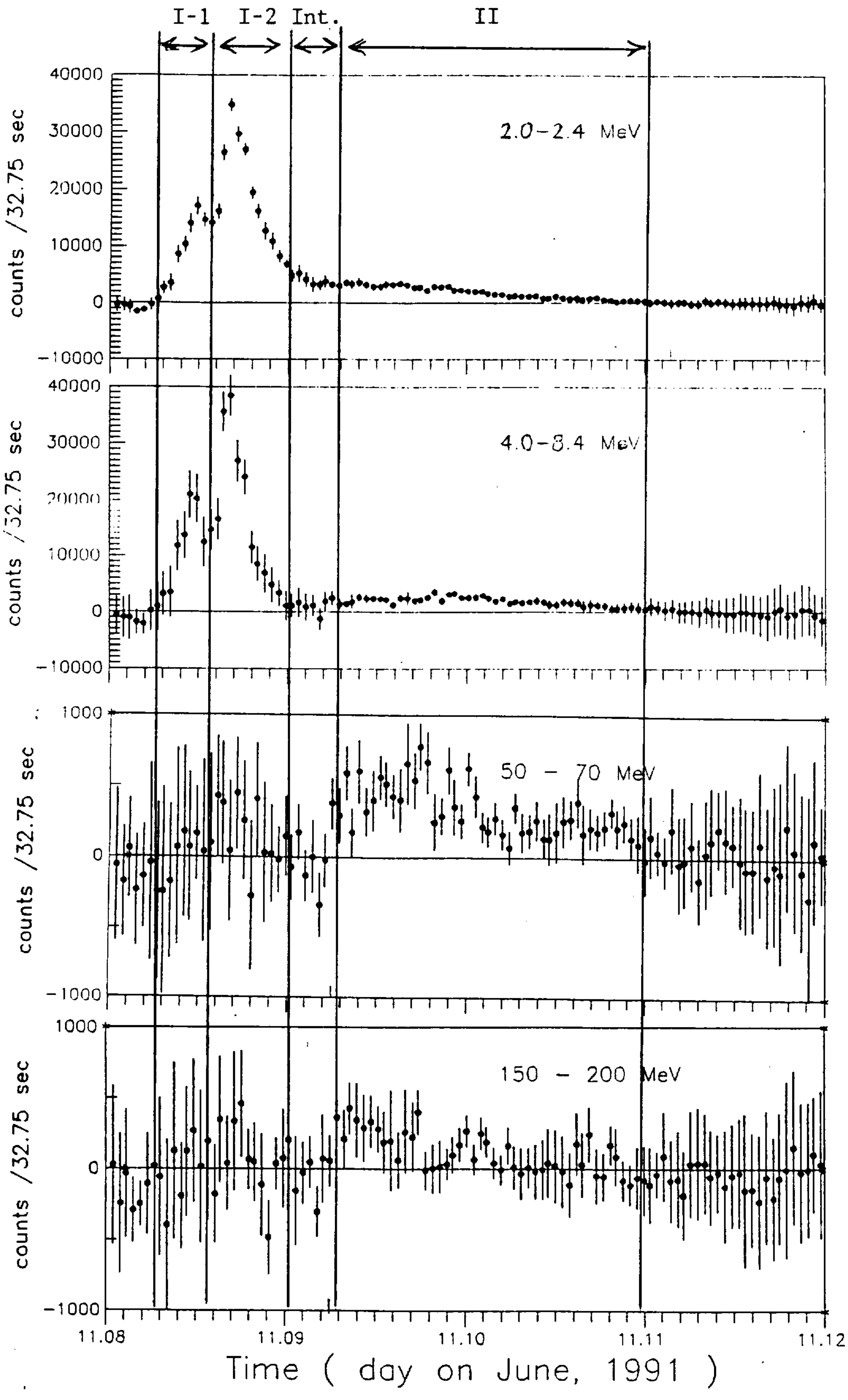

I-1
I-2
Int.
II
2.0-2.4 MeV
4.0-8.4 MeV
50 - 70 MeV
150 - 200 MeV
counts /32.75 sec
40000
30000
20000
10000
0
-10000
1000
-1000
11.08
11.09
11.10
11.11
11.12
Time (day on June, 1991)

Figure 2.

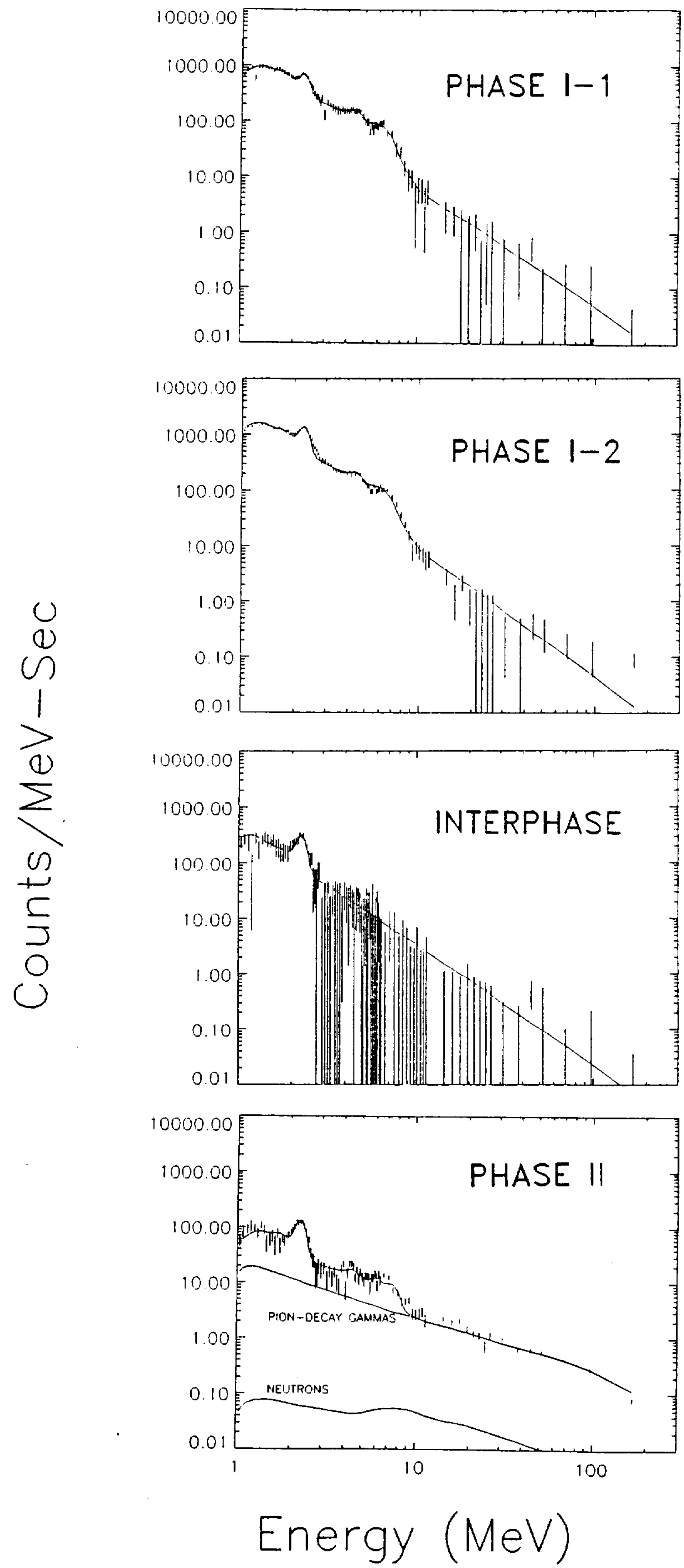
PHASE I-1
PHASE I-2
INTERPHASE
PHASE II
PION-DECAY GAMMAS
NEUTRONS
Counts/MeV-Sec
Energy (MeV)
10000.00
1000.00
100.00
10.00
1.00
0.10
0.01
1
10
100

Figure 3.

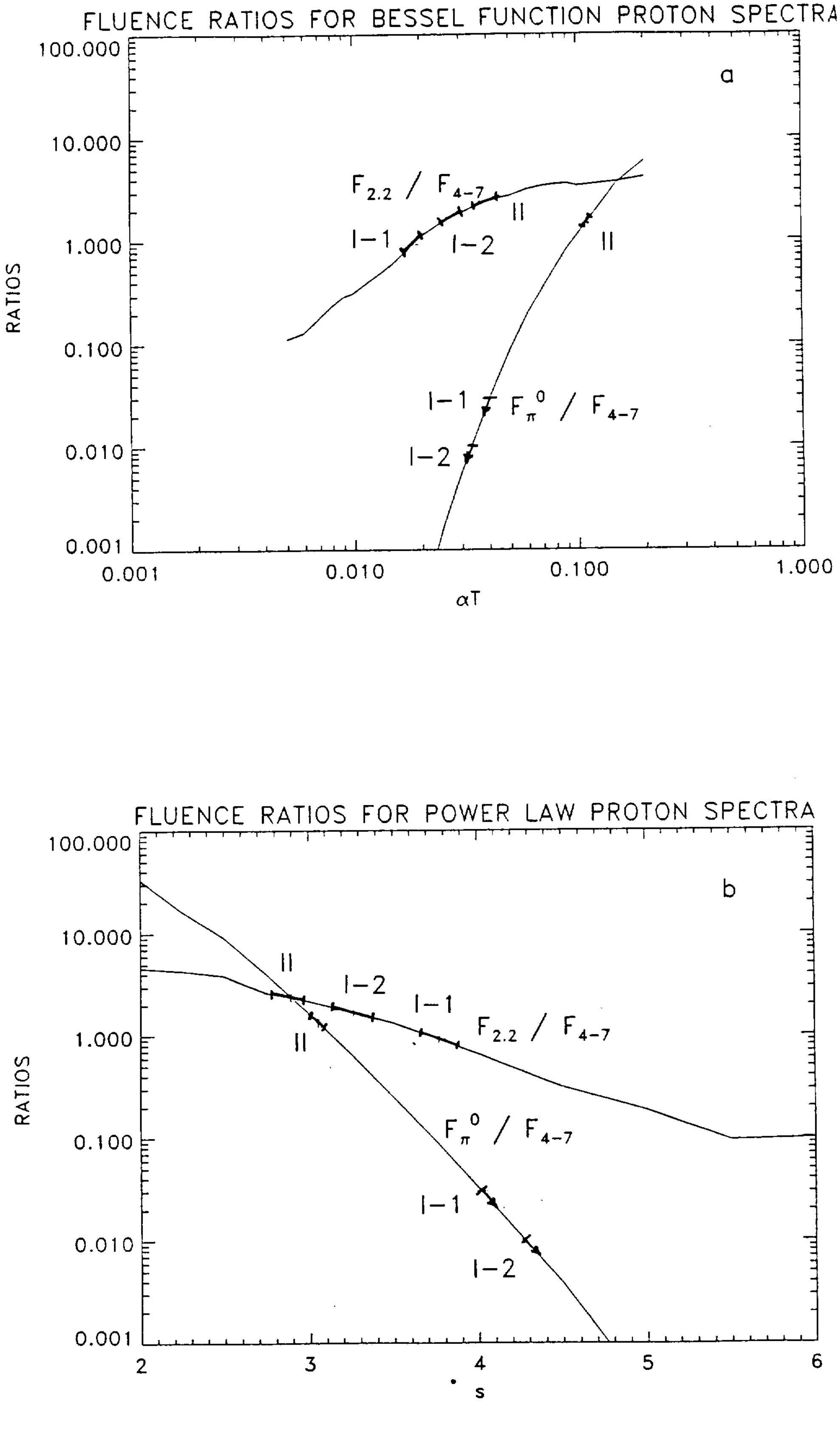
FLUENCE RATIOS FOR BESSEL FUNCTION PROTON SPECTRA
a
RATIOS
αT
$F_{2.2}$ / F_{4-7}
$F_{\pi}{}^{0}$ / F_{4-7}
I-1
I-2
II
FLUENCE RATIOS FOR POWER LAW PROTON SPECTRA
b
RATIOS
s
$F_{2.2}$ / F_{4-7}
$F_{\pi}{}^{0}$ / F_{4-7}
I-1
I-2
II

Figure 4.